advances
in radiation oncology

Scientific Article

Kilovoltage projection streaming-based tracking application (KiPSTA): First clinical implementation during spine stereotactic radiation surgery

Jihun Kim PhD [a,b], Yang-Kyun Park PhD [c], David Edmunds PhD [b], Kevin Oh MD [b], Gregory C. Sharp PhD [b], Brian Winey PhD [b,*]

[a] *Department of Radiation Oncology, Yonsei Cancer Center, Seoul, South Korea*
[b] *Department of Radiation Oncology, Massachusetts General Hospital and Harvard Medical School, Boston, Massachusetts*
[c] *Department of Radiation Oncology, University of Texas Southwestern Medical Center, Dallas, Texas*

Abstract

Purpose: This study aimed to develop a linac-mounted kilovoltage (kV) projection streaming-based tracking method for vertebral targets during spine stereotactic radiation surgery and evaluate the clinical feasibility of the proposed spine tracking method.

Methods and materials: Using real-time kV projection streaming within XVI (Elekta XVI), kV–projection-based tracking was applied to the target vertebral bodies. Two-dimensional in-plane patient translation was calculated via an image registration between digitally reconstructed radiographs (DRRs) and kV projections. DRR was generated from the cone beam computed tomography (CBCT) scan, which was obtained immediately before the tracking session. During a tracking session, each kV projection was streamed for an intensity gradient-based image with similar metric-based registration to the offset DRR. The ground truth displacement for each kV beam angle was calculated at the beam isocenter using the 6 degrees-of-freedom transformation that was obtained by a CBCT-CBCT rigid registration. The resulting translation by the DRR-projection registration was compared with the ground truth displacement. The proposed tracking method was evaluated retrospectively and online, using 7 and 5 spine patients, respectively.

Results: The accuracy and precision of spine tracking for in-plane patient motion were 0.5 ± 0.2 and 0.2 ± 0.1 mm. The magnitude of patient motion that was estimated using the CBCT-CBCT rigid registration was $(0.5 \pm 0.4, 0.4 \pm 0.3, 0.3 \pm 0.3)$ mm and $(0.3 \pm 0.4, 0.2 \pm 0.2, 0.5 \pm 0.6)$ mm for all tracking sessions. The intrafraction motion was within 2 mm for all CBCT scans considered.

Conclusions: This study demonstrated that the proposed spine tracking method can track intrafraction motion with sub-millimeter accuracy and precision, and sub-second latency.

Introduction

High-dose, per fraction, radiation therapy is a rapidly emerging ablative therapy for the management of spinal metastases.[1-4] The goal is to deliver a high radiation dose to a tumor volume in a limited number of fractions (eg, single fraction in stereotactic radiation surgery [SRS]) and 2 to 5 fractions in stereotactic body radiation therapy while maintaining the dose to normal tissue at a safe level. The main advantages of using higher doses per fraction are the increased biologically equivalent dose and reduced treatment time but require highly conformal dose distributions to avoid normal tissue complications.

In spine SRS, highly conformal doses to a target volume can be achieved by advanced treatment techniques such as intensity modulated radiation therapy (IMRT), robotic radiation therapy, and volumetric modulated radiation therapy (VMAT). Although the use of IMRT[5,6] and robotic radiation surgery (CyberKnife)[7,8] for spine cancer treatment has been well established, VMAT treatment has emerged only recently.[9-13] One treatment platform was reportedly not dosimetrically favored over others between IMRT, robotic radiation surgery, and VMAT.[11-13]

However, the treatment quality of spine SRS with steep dose gradients may be reduced by intrafraction patient motion. Loss of target coverage and overdose to organs at risk have been reported in previous studies.[14-16] Because of the low tolerance of the spinal cord to radiation[17-19] and high dose gradients in proximity to the spinal cord, appropriate motion management during spine stereotactic radiation therapy is essential to improve treatment quality. CyberKnife, the first treatment system for motion-adaptive radiation therapy, is capable of tracking tumors with 2 kV x-ray tubes and an optical tracking system and adapting to intrafraction patient motion using nonisocentric beam arrangements.[20] Cone beam computed tomography (CBCT) is the standard imaging guidance for most linac-based, hypofractionated radiation therapy. However, the previous study[21] reported that large patient motions (eg, >2 mm; >2°) occasionally occurred between CBCT acquisitions (initial setup, verification, midtreatment, and posttreatment CBCTs) for spine SRS treatment, which indicates the need for real-time tracking.

Recently, kV projection imaging-based monitoring techniques have been explored for positional verification of patients with spine cancer.[22,23] Verbakel et al. monitored the spine position by comparing digital tomosynthesis images and planning computed tomography. Hazelaar et al.[23] employed a 2-dimensional template, matching-based method

and retrospectively analyzed 18 patients who received spine stereotactic body radiation therapy. For each gantry angle, a 2-dimensional offset was calculated via a template that matched between template and kV projection. The template was a sub-region of a digitally reconstructed radiograph that was generated from planning computed tomography (pCT) including a contoured vertebra with a margin. However, Hazelaar et al.[23] demonstrated the feasibility of the kV-projection-based spine by monitoring only in a retrospective manner.

In this study, a real-time spine tracking method was developed and implemented with an in-house software package using projections that were streamed from a commercially available linac-mounted imaging system. The spine tracking method was based on image registration between digitally reconstructed radiographs and kV projection. An image gradient-based similarity metric was used for the image registration.

Methods and materials

Clinical implementation of kV projection streaming-based tracking application

A spine tracking method was implemented with an in-house software package called the kV projection streaming-based tracking application (KiPSTA). The development of the intrafraction spine tracking was based on the capability of Elekta XVI software (Elekta Synergy, XVI version 5, Elekta AB, Stockholm, Sweden) to stream kV projection images. The software performs 2-dimensional image registrations between digitally reconstructed radiograph (DRR) images and kV projection images to measure inplane translations of the patient. Herein, the authors detail each step in the spine tracking algorithm and Figure 1 shows the graphical user interface of KiPSTA.

KiPSTA was tested online on 5 spine SRS patients, and a retrospective analysis was performed on 7 patients (12 consecutive patients total). Spine tracking was performed between any 2 consecutive CBCT scans ($CBCT_n$ and $CBCT_{n+1}$), which resulted in ($N-1$) tracking sessions for each patient, where $CBCT_n$ represents the n-th CBCT scan ($n = 1, …, N$-1) and N is the number of CBCT scans. For instance, if the first tracking session is performed between the first and second CBCT scans, and if 4 CBCT scans are obtained for a patient, the final (third) tracking session is between the third and fourth CBCT scans.

In total, tracking was performed for 28 CBCT scans using KiPSTA: 20 retrospective and 8 online tracking sessions.

Figure 1 Graphical user interface of KiPSTA. For spine tracking, KiPSTA displays the following: 1) comparison between DRR and kV projection, and 2) position error (color-coded green box turns red when the detected error is larger than a threshold). Of note, KiPSTA was developed for multiple tracking modes including fiducial marker and diaphragm tracking although only data relevant to spine tracking is displayed.

The positional uncertainty that was calculated by KiPSTA was categorized into verification (15 fractions) and intrafraction (13 fractions). Intrafraction residual error represents the positional uncertainty that mainly stems from patient motion during treatment (ie, positional uncertainty detected between a CBCT scan immediately before treatment and a subsequent mid-treatment CBCT scan). On the other hand, verification residual error was defined as the positional uncertainty detected between CBCT scans that are obtained to further verify the patient position either prior to or in the middle of treatment.

All patients in this study were treated by single-fraction VMAT (2 or 3 arcs) using an Elekta Agility linear accelerator. For patient setup, patients were localized using the on-board CBCT imaging, and patients were immobilized using Vac-Lok Bag (Civco, Coralville, IA). A thermoplastic mask was used for patients in whom the target volume existed in the region of cervical spine or upper thoracic spine. For most patients, 2 pretreatment CBCT scans (median: 2; maximum: 4) and 1 midtreatment CBCT scan (median: 1; maximum: 3) were acquired.

KiPSTA was installed and run on a standard PC (Windows 7, Intel Core i7-2600 CPU, 3.40 GHz, 8 GB RAM). Latency, which can be defined as the time between beam exposure and display of tracking results, was approximately 700 ms including beam exposure, projection streaming, and image processing. The time spent to respond to the tracking results (ie, manually stop the beam delivery after a movement that was larger than the tolerance observed) was not included because this can be user-dependent. Because kV projections were streamed with a frame rate of approximately 5 frames, spine tracking was performed approximately for every 4 projections. Of note, the tracking results were calculated for a single projection, not averaging over the multiple projections that were acquired during the time delay. Although there was no additional imaging dose to patients in the current study of spine tracking, the imaging dose per total rotational scan was measured at approximately 1 cGy computed tomography dose index, with 1 mAs per projection for thoracic and lumbar spine imaging protocols. For cervical spine imaging protocols, the total scan dose (ie, computed tomography dose

index) was measured at 0.1 cGy per scan with 0.1 mAs per projection.

Preprocessing prior to spine tracking

First, the patient data set (planning computed tomography, treatment plan, and contours) was transferred to the computer where KiPSTA was installed. Second, a point of interest was set to be a geometric center of planning target volume (PTV), which was calculated by averaging the coordinates of the points that comprised the PTV structure. Then, a 300×300-pixel region of interest (ROI) that was centered on the point of interest was defined. The size of the ROI was approximately 76×76 mm^2 because the pixel size of the raw kV projections was 0.39 mm on the detector (0.25 mm at isocenter). This ROI confined the DRR generation to a region that encompassed the target vertebral bodies.

## Projection streaming and digitally reconstructed radiograph

The overall workflow of the spine tracking method in KiPSTA is summarized in Figure 2. A set of projections PROJ$_n$ was transmitted to KiPSTA via a projection-streaming client. For each CBCT scan, approximately 300 projections were acquired and the image registration was performed for each. Using the streamed projections, a CBCT image was reconstructed.

The CBCT reconstruction was performed with a voxel size of 1 mm in all directions using a standard Feldcamp-Davis-Kress cone beam reconstruction algorithm (Hann and HannY filters with a cutoff frequency of 5.0) in the Reconstruction Toolkit, an open-source software.[24] The original kV projections had an image dimension of 1024×1024 pixels, but were down-sampled by a factor of 2 to reduce the reconstruction time. The reconstructed CBCT image has a 1 mm pixel dimension for all directions. The kV projections were acquired using an Elekta XVI system with 100 kVp tube voltage, 10 mA tube current, 10 ms exposure time, and 5 fps frame rate. The XVI panel sag, which was streamed with the projection image, was applied to correct to the position of the kV projections.

The reconstructed CBCT image was transformed using a 6 degree-of-freedom (DOF) couch correction vector that was obtained with an automatic rigid registration from XVI. The transformed CBCT image (CBCT$_{n,txpos}$) represents the patient geometry aligned for radiation treatment. The translation and rotation that are calculated by the automatic rigid registration were manually entered into KiPSTA.

As another set of kV projections (PROJ$_{n+1}$) was streamed, DRR$_n$ was generated from CBCT$_{n,txpos}$ for each gantry angle using the predefined ROI$_n$. This forward projection was performed using the Reconstruction Toolkit with the beam geometry of the on-board CBCT imaging system (source-axis distance = 1000 mm; source-detector
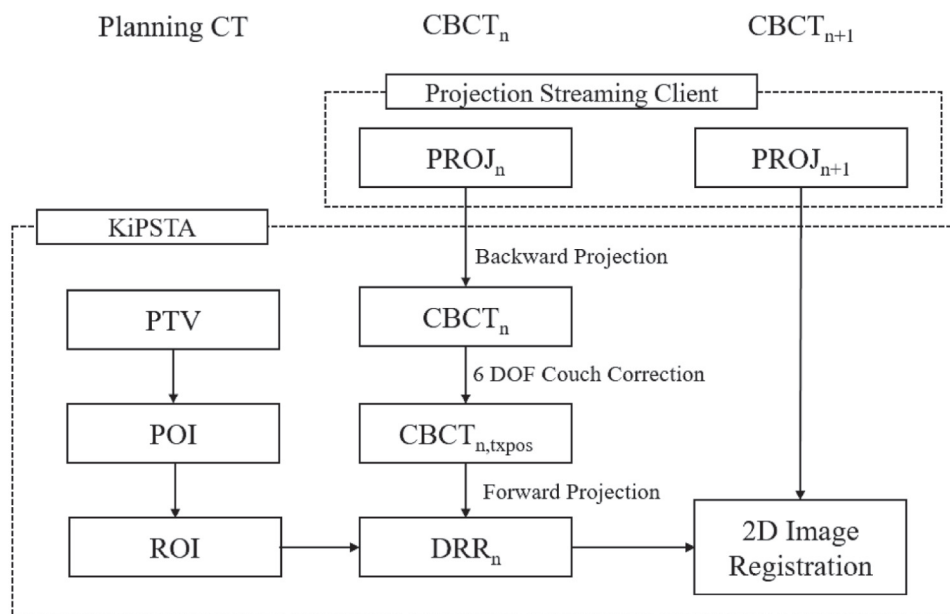
Figure 2 Workflow of spine tracking between *n*-th and (*n*+1)-th CBCT scans, CBCT$_n$ and CBCT$_{n+1}$. PTV, planning target volume; POI, point of interest; PROJ, projection; ROI, region of interest; txpos, treatment position. PTV was used to calculate the POI, which is the mean of the PTV contours points. The ROI, in which the 2-dimensional image registration was performed, was calculated using the POI. For the *n*-th spine tracking, CBCT$_{n,txpos}$ was considered the reference image from which digitally reconstructed radiographs were generated. CBCT$_{n,txpos}$ was generated by applying 6 degree-of-freedom couch corrections to CBCT$_n$.

distance = 1536 mm) so that the resulting DRRs had the same scale as the kV projections. Although previous studies used planning computed tomography images as reference images, the authors used daily CBCT images for reference DRR generation for the following reasons: 1) The daily CBCT better represents the patient anatomy on the treatment day, which can be considered the baseline for intrafractional motion; and 2) in our preliminary investigation, the registration between CBCT-based DRR and kV projection demonstrated better performance over the registration between planning computed tomography DRR and kV projections.

Digitally reconstructed radiograph-projection image registration

Prior to image registration, a median filtering with a window size of 3 was applied to the DRRs and kV projections to reduce the noise level. Image registration was performed to calculate in-plane patient translation (ie, 2-dimensional translation in rotating plane orthogonal to the kV beam direction). The DRR-projection image registration was mathematically formulated to find an optimal 2-dimensional translation to maximize an intensity gradient-based image with similar metric. In the implementation of this image with similar metric by the Insight Segmentation and Registration Toolkit,[25] the sum of the squared difference in the image gradients was minimized between 2 images. This Insight Segmentation and Registration Toolkit implementation of the image with similar metric was based on the gradient difference metric described by Hipwell et al. in Appendix F.[26]

The image registration was performed for each set of DRR and kV projection, which resulted in 2-dimensional translation vector $d_{KiPSTA}(\varphi)$ where φ represents the projection angle. As explained, the ROI for the image registration was defined as a square of 300×300 pixels, where the center is the mean of the PTV contour points.

Evaluation of spine tracking accuracy

To evaluate the spine tracking accuracy (ie, accuracy of the 2-dimensional image registration), ground truth translation $d_{ref}(\varphi)$ was calculated by performing 3-dimensional $CBCT_n$-$CBCT_{n+1}$ registrations using Plastimatch,[27] an open-source software for image computation. A single-resolution image registration was performed between each set of CBCTs, $CBCT_n$ and $CBCT_{n+1}$. The ROI, where the mean squared error of image intensity was calculated, was confined to a 3-dimensional rectangular region that encompassed the PTV. The resulting rotation matrix by the 3-dimensional CBCT-CBCT registration was used to calculate a 3-dimensional displacement vector at the isocenter and this displacement, vector $d_{iso}(\varphi)$, was projected to each kV beam plane, which resulted in the ground truth, in-plane translation as follows:

$$d_{ref}(\varphi) = d_{iso}(\varphi) - (d_{iso}(\varphi) \cdot e_\perp) e_\perp \quad (1)$$

where $e_\perp$ represents the unit vector orthogonal to the beam plane. The spine tracking error $e(\varphi)$ was calculated as the absolute difference between the ground truth translation vector $d_{ref}(\varphi)$ and the one tracked by the 2-dimensional registration of KiPSTA, $d_{KiPSTA}(\varphi)$, as follows:

$$e(\varphi) = d_{KiPSTA}(\varphi) - d_{ref}(\varphi) \quad (2)$$

For each tracking session, mean and standard deviation (SD) were calculated from the absolute registration errors across the kV beam angles, representing the accuracy and precision of the spine tracking. The impact of the following 4 parameters on the spine tracking accuracy (2-dimensional vector magnitude) was investigated: (1) type of residual error (verification, intrafraction); (2) tumor site (cervical, thoracic, and lumbar); (3) spinal implant (yes/no); and (4) tracking mode (online or retrospective).

Comparisons were made by dividing 28 tracking sessions into 2 or 3 groups and performing an unpaired two-sample t test (MATLAB t test2). With regard to the tumor site for instance, the tracking results for the thoracic spine (12 sessions) and lumbar spine (7 sessions) were compared with those for the cervical spine (9 sessions). Using the t test, the result was tested if 2 different samples were statistically different with a 95% significance level ($P < .05$). The significance of the difference in patient motion (6 DOF transformation), calculated by the CBCT-CBCT registration, was also tested between each of the 2 groups using the t test.

To investigate the angular dependency of the accuracy and precision, the 2-dimensional vector magnitude of the tracking error was compared between the 2 angular groups: lateral (45-135° and 225-315°) and anteroposterior (0-45°, 135-225°, and 315-360°) kV beam angles. This comparison was performed using a paired t test (MATLAB t test) for each tumor site.

Of note, the purpose of calculating these statistics is not to draw strong conclusions on the impact of the parameters considered. Rather, the statistical analysis was performed to provide details of the tracking results. Comparing the tracking errors between the groups can examine if the spine tracking algorithm does not appropriately perform under certain conditions.
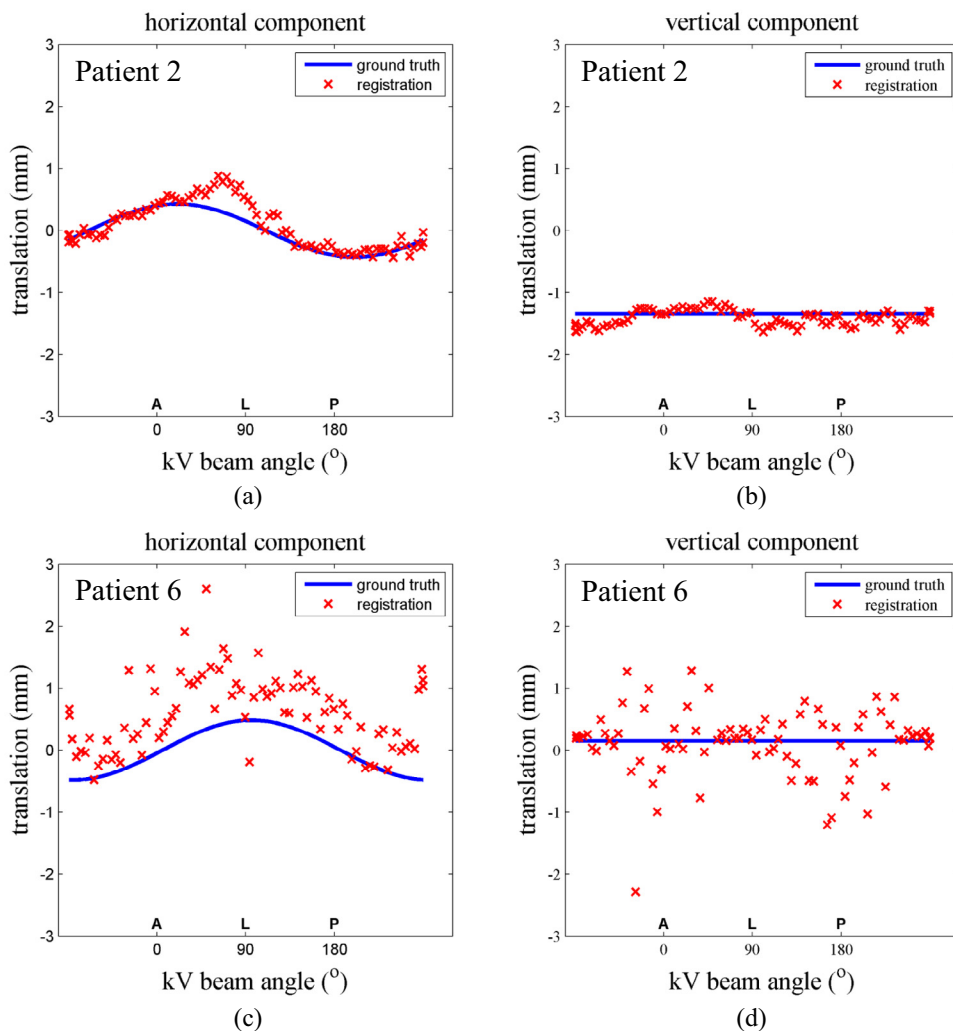
Results

Table 1 summarizes the statistics (mean and SD) of the absolute tracking errors calculated over the kV beam angles for each tracking session and the ground truth 6 DOF transformation obtained by the CBCT-CBCT registrations. The mean of the absolute tracking error was <1.0 mm for all

Table 1 Summary of statistics of absolute tracking error by DRR-kV projection registration and ground truth 6 DOF transformation by CBCT-CBCT registration

Patient no.	Tracking no. n	Absolute tracking error (mm)				Ground truth 6 DOF transformation (CBCT$_n$-CBCT$_{n+1}$ registration)						Type of residual error	Online	Tumor site	Implant
		Horizontal	Vertical	2D Vector	>1 mm (%)	Translation (mm)			Rotation (°)						
						x	y	z	x	y	z				
mean		0.3 ± 0.2	0.3 ± 0.2	0.5 ± 0.2	4.1	0.5	0.4	0.3	0.3	0.2	0.6				
SD		0.1 ± 0.1	0.1 ± 0.1	0.2 ± 0.1	6.9	0.4	0.3	0.3	0.4	0.2	0.6				
1	1	0.2 ± 0.1	0.2 ± 0.1	0.3 ± 0.1	0.0	1.8	−0.3	−0.7	−0.4	−0.3	1.1	Verification	No	C2	Yes
	2	0.3 ± 0.2	0.5 ± 0.2	0.6 ± 0.2	2.1	−0.7	−1.5	−0.3	−1.5	0.4	0.4	Intrafraction	No		
	3	0.2 ± 0.2	0.1 ± 0.1	0.3 ± 0.2	0.0	0.3	0.5	−0.3	0.6	−0.1	0.0	Verification	No		
	4	0.2 ± 0.1	0.2 ± 0.1	0.3 ± 0.1	0.0	−0.7	−0.4	−0.1	0.0	0.4	0.3	Intrafraction	No		
2	1	0.1 ± 0.1	0.1 ± 0.1	0.2 ± 0.1	0.0	0.4	0.2	−1.3	0.5	0.1	0.1	Verification	No	L4-5	Yes
	2	0.2 ± 0.2	0.1 ± 0.1	0.3 ± 0.2	0.0	0.0	0.0	0.0	0.3	−0.1	−0.4	Verification	No		
	3	0.2 ± 0.2	0.1 ± 0.1	0.3 ± 0.1	0.0	0.0	0.5	−0.9	0.6	0.0	0.6	Intrafraction	No		
3	1	0.5 ± 0.3	0.2 ± 0.1	0.6 ± 0.3	11.0	0.2	0.3	−0.1	−0.3	0.4	0.6	Verification	No	T9	Yes
	2	0.5 ± 0.3	0.2 ± 0.2	0.6 ± 0.3	10.5	−0.3	−0.1	0.0	−0.2	−0.4	−0.1	Intrafraction	No		
4	1	0.2 ± 0.2	0.1 ± 0.1	0.3 ± 0.2	0.0	0.5	0.3	−0.3	0.1	−0.1	−0.4	Verification	No	C2	No
	2	0.5 ± 0.3	0.2 ± 0.1	0.5 ± 0.3	8.5	0.9	0.2	0.1	0.8	−1.0	−0.8	Intrafraction	No		
5	1	0.5 ± 0.2	0.2 ± 0.2	0.6 ± 0.2	5.5	0.3	0.3	−0.6	−0.3	−0.2	0.5	Verification	No	T9-10	Yes
	2	0.3 ± 0.2	0.3 ± 0.2	0.4 ± 0.2	1.2	0.6	−0.1	−0.2	0.0	−0.2	−0.4	Intrafraction	Yes		
6	1	0.6 ± 0.4	0.4 ± 0.3	0.7 ± 0.4	22.4	−0.8	0.0	0.4	0.3	0.0	−0.6	Verification	No	T7-8	No
	2	0.6 ± 0.5	0.4 ± 0.5	0.8 ± 0.6	27.1	0.0	0.5	0.1	−0.1	−0.1	−0.4	Intrafraction	No		
7	1	0.3 ± 0.3	0.5 ± 0.3	0.6 ± 0.3	10.4	0.2	−0.9	0.4	1.4	0.0	0.2	Intrafraction	No	T1	No
	2	0.2 ± 0.2	0.1 ± 0.1	0.3 ± 0.3	1.9	0.0	−0.7	0.3	0.4	−0.2	−0.2	Verification	No		
8	1	0.3 ± 0.2	0.4 ± 0.2	0.5 ± 0.3	4.9	−0.7	−0.8	0.1	0.1	0.2	−0.5	Verification	Yes	C6	Yes
	2	0.2 ± 0.2	0.4 ± 0.2	0.5 ± 0.2	0.0	−0.1	−0.3	0.1	0.1	0.1	0.7	Verification	Yes		
	3	0.5 ± 0.1	0.1 ± 0.1	0.5 ± 0.1	0.0	−0.8	−0.4	0.0	0.0	0.1	0.1	Intrafraction	No		
9	1	0.3 ± 0.2	0.5 ± 0.1	0.6 ± 0.2	1.2	0.9	0.0	−0.4	−0.1	0.1	−0.7	Verification	Yes	L1-2	Yes
	2	0.2 ± 0.1	0.5 ± 0.1	0.6 ± 0.2	0.0	0.8	0.5	−0.7	−0.1	0.0	0.1	Intrafraction	Yes		
10	1	0.2 ± 0.2	0.3 ± 0.2	0.5 ± 0.1	0.0	−0.4	−0.4	0.0	−0.1	0.3	0.3	Verification	Yes	L1	Yes
	2	0.4 ± 0.2	0.2 ± 0.1	0.5 ± 0.2	0.0	−0.3	−0.4	0.2	−0.1	0.5	−0.6	Intrafraction	No		
11	1	0.5 ± 0.3	0.2 ± 0.1	0.6 ± 0.3	3.6	−0.5	−0.3	−0.3	0.1	0.1	−2.7	Verification	No	T10-11	Yes
	2	0.4 ± 0.3	0.2 ± 0.2	0.5 ± 0.2	3.3	1.2	0.2	−0.1	0.1	0.7	2.0	Intrafraction	No		
12	1	0.4 ± 0.2	0.2 ± 0.2	0.5 ± 0.2	0.0	−0.8	0.3	0.2	0.2	0.0	−0.4	Verification	Yes	T9-10	Yes
	2	0.3 ± 0.2	0.2 ± 0.1	0.4 ± 0.1	0.0	0.1	0.1	0.0	0.0	0.0	0.4	Intrafraction	Yes		

2D, 2-dimensional; CBCT, cone beam computed tomography; DOF, degree of freedom; no, number; DRR, digitally reconstructed radiograph; SD, standard deviation.

Mean and SD of absolute 6 DOF transformation were calculated. Horizontal and vertical directions for the 2-dimensional registration error represent left-right and bottom-top directions from the kV imaging beam's eye view. For the 3-dimensional registration, the x, y, and z directions represent right-left, anterior-posterior, and inferior-superior directions, respectively.

Figure 3 Comparisons of 2-dimensional ground truth translation and resulting translation for (A), (B) patient 2 (lumbar), and (C), (D) patient 6 (thoracic). Horizontal component ((A), (C)) and vertical component ((B), (D)) of the translations were plotted separately. A, anterior; P, posterior; L, left.

tracking sessions, which demonstrates sub-millimeter accuracy of KiPSTA for spine tracking. The mean and SD of the mean absolute tracking error (vector) across the patient cohort was 0.5 ± 0.2 mm. The percentage of the angles, for which the absolute tracking error was >1 mm, was <10% for all cervical and lumbar spine patients. On the other hand, the percentage was larger for thoracic spine patients with the maximum percentage at 27.1% for patient 6 (no spinal implant).

The patient translation and rotation (mean $\pm$ SD of absolute motion across the tracking sessions) were 0.5 ± 0.4, 0.4 ± 0.3, 0.3 ± 0.3 mm and 0.3 ± 0.4, 0.2 ± 0.2, $0.6 \pm 0.6°$ in the x (right-left), y (anterior-posterior), and z (inferior-superior) directions, respectively. The maximum translation and rotation were 1.8, 1.5, and 1.3 mm and 1.5, 1.0, 2.7° in each direction, respectively. The translation was within 2 mm in all cases. For 1 of 28 cases (3.6%), the rotation was >2° about the inferior-superior axis.

Figure 3 shows the comparisons between the ground truth and tracked translations for patients 2 (CBCT1-CBCT2) and 6 (CBCT2-CBCT3), in which minimum and maximum absolute registration errors were observed: 0.2 ± 0.1 mm versus 0.8 ± 0.6 mm. While the registration errors were within 1 mm for patient 2 (lumbar), those for patient 6 (thoracic) were relatively large across the kV beam angles, which resulted in registration errors >1 mm for 27.1% of the beam angles. The corresponding 6 DOF transformations that were obtained by the CBCT-CBCT registration were 0.4, 0.2, and -1.3 mm and 0.5, 0.1, and 0.1° versus 0.0, 0.5, and 0.1 mm and -0.1, -0.1, and 0.4°.

Between each of the 2 groups divided by the chosen parameters, the patient motion was statistically similar except for the rotation about the x axis (right-left) for the online versus retrospective residual errors. The mean magnitude of the right-left rotation was 0.4° for the retrospective cases and 0.1° for the online cases ($P = .04$).
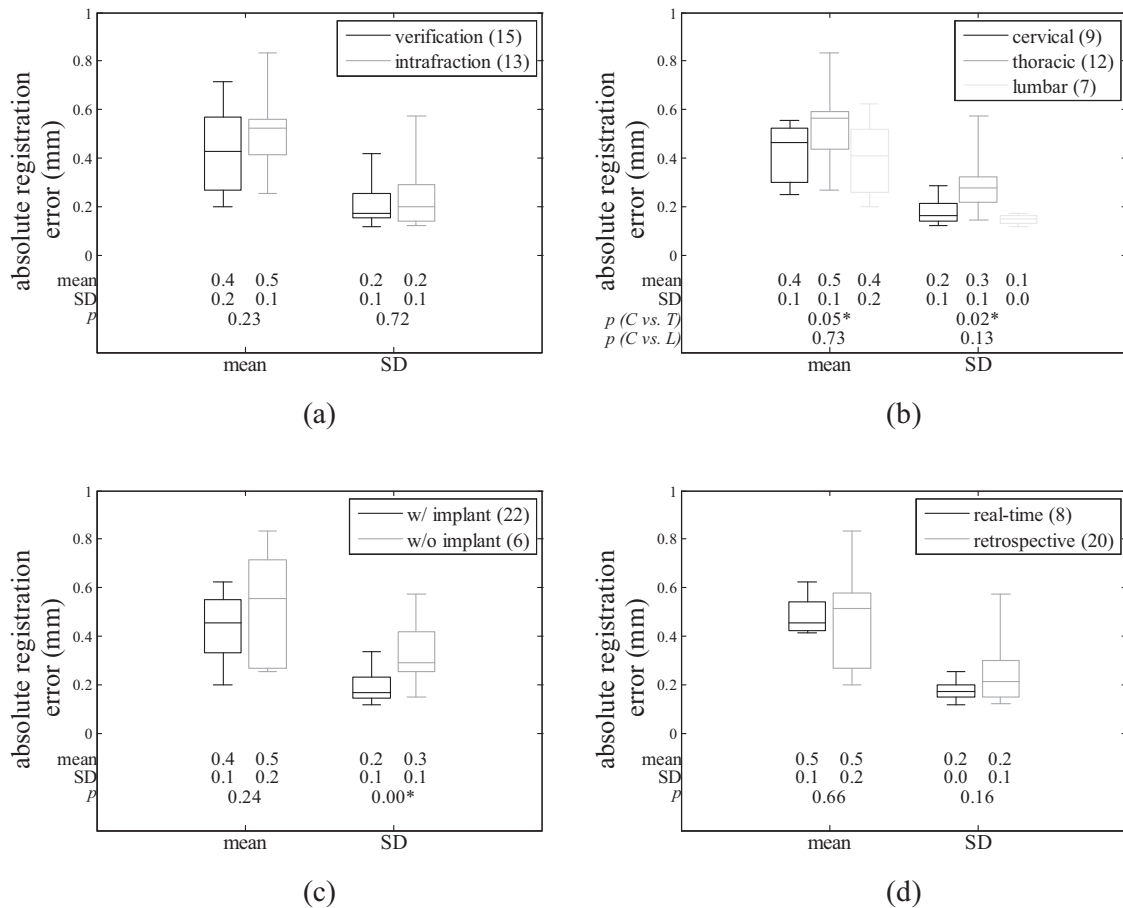
Figure 4 Comparisons of box plots of mean and standard deviation of absolute tracking error, calculated across kV beam angles and showing distributions across tracking sessions as well as the impact of different parameters: (A) type of residual error, (B) tumor site, (C) spinal implant, and (D) tracking mode. *95% statistical significance of difference between data by an unpaired *t* test.

Figure 4 shows the impact of the 4 different parameters on the tracking accuracy in the form of a boxplot (mean, minimum, maximum, and 25% and 75% quantiles) with mean and SD across the tracking sessions, and *P*-value for a 95% statistical significance of difference. The spine tracking accuracy was not significantly affected by type of residual error and tracking mode (Figs 4A and D). The accuracy and precision of spine tracking were significantly lower for thoracic patients than those for cervical spine patients. The precision of spine tracking was the highest for lumbar spine patients as indicated by a narrow distribution of the SD in Figure 4B. The precision of spine tracking was significantly better for patients with spinal implants than for those without (*P* = .002).

Some angular dependency was seen for thoracic and lumbar spine patients although the difference in the accuracy and precision was small (<0.1 mm) between the lateral and anteroposterior angles (Fig 5). Only the mean of the vector magnitude of the tracking error for lumbar spine patients was significantly different between the lateral and anteroposterior angles. For thoracic and lumbar patients, the *P*-values that compared the SD between the lateral and

anteroposterior angles were .06 and .08, which indicates marginal significance of difference; thus, higher accuracy and precision were achieved for the anteroposterior than the lateral angles.

Discussion

A kV projection streaming-based spine tracking method was developed and clinically implemented in our KiPSTA software package. Its sub-millimeter accuracy and precision, and sub-second latency were demonstrated in online implementation, which indicates the clinical feasibility of the spine tracking method. KiPSTA can be immediately used to capture any abrupt spine patient motion between CBCT scans although follow-up investigations will be required.

A limitation of this study is that the kV projections were acquired with the mega-voltage beam turned off; therefore, the intrafraction patient motion was not monitored in real-time but online with a time delay. Since projections can be streamed during gantry rotations, KiPSTA will be most beneficial when kV projections are acquired during
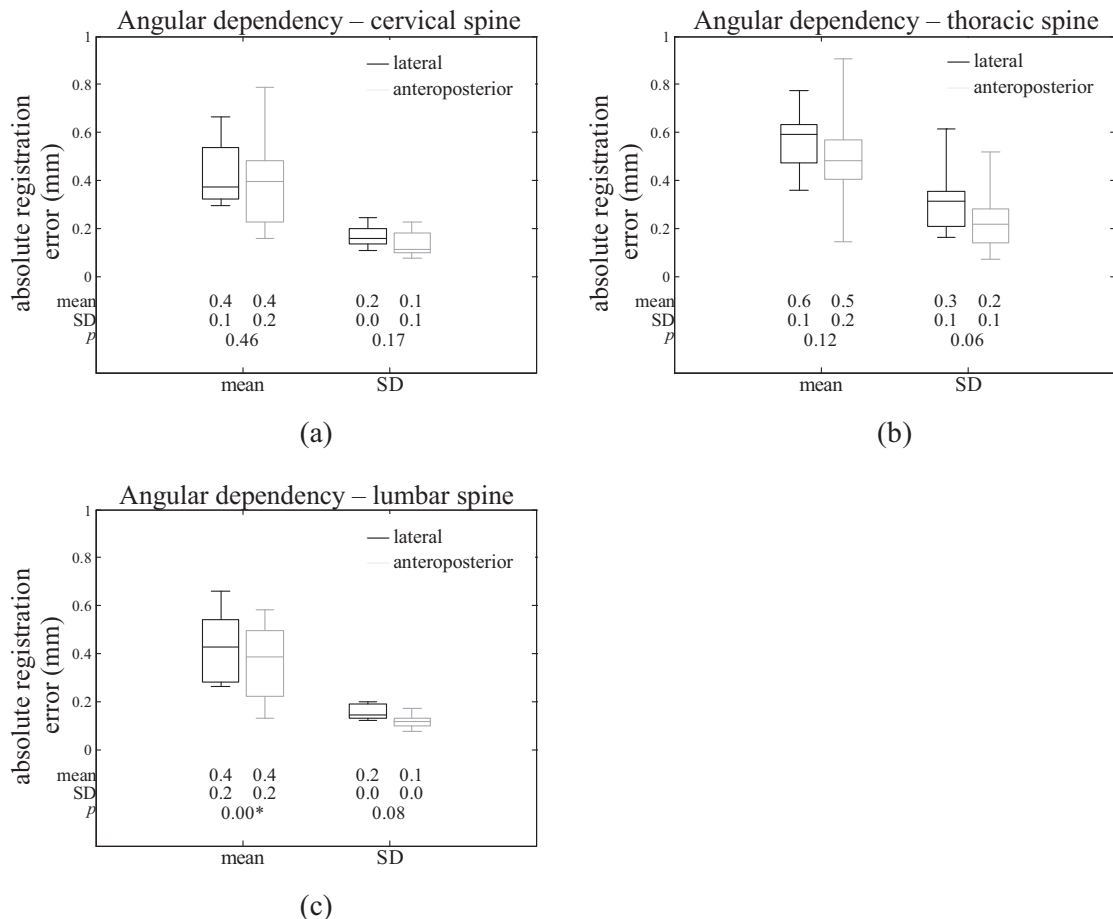
Figure 5 Comparisons of box plots of mean and standard deviation of absolute tracking error, calculated across kV beam angles and showing distributions across tracking sessions as well as angular dependency (lateral vs anteroposterior) of the tracking error for (A) cervical, (B) thoracic, and (C) lumbar spine patients. *95% statistical significance of difference between data by a paired *t* test.

VMAT delivery, but further study is needed to mitigate the image-quality degradation from mega-voltage scatter. The beam delivery can be stopped manually by the operator when a patient motion that is detected by KiPSTA is larger than a predefined limit (eg, 3 mm). This threshold value can be selected on the basis of the study by Wang et al.[15]

The current version of KiPSTA could be useful also for IMRT where kV projection images are acquired between consecutive static beam angles. The proposed spine tracking method can be supplemented with a surrogate tracking method such as optical tracking. The image quality of CBCT scans that are concomitantly acquired with mega-voltage treatment beam is generally degraded due to mega-voltage scatter from patients.[28] Because the degraded image quality in the intrafraction kV projections can result in reduced tracking accuracy, spine tracking using the intrafraction kV imaging should be investigated in a future study.

Two-dimensional patient movement was calculated from the proposed spine tracking method. Estimating 3-dimensional patient movement from the translations calculated may be possible for several angles as suggested in

Hazelaar et al.[23] This estimation of a 3-dimensioinal motion can provide average motions during a certain period of time for kV projection acquisitions and may improve the robustness of the spine tracking method to the registration uncertainty across kV projection angles.

All patient motions that were detected by KiPSTA were within 3 mm, which indicates that patient movement was moderate and a relatively long treatment time was well tolerated by the patient cohort. Also, the mean and SD of the patient motions that were calculated by the CBCT-CBCT registration was comparable with those reported in the previous study,[21] with a 95% confidence interval of absolute translation and rotation motions of 1.2 mm and 0.9° in Hyde et al. Although no noticeable movement was observed in the patient cohort, monitoring patient movement during spine SRS remains of paramount importance. There is the potential for discomfort that is caused by spinal implants combined with the relatively long treatment time for large patient movements. Of note, the CBCT-CBCT registration error is negligible compared with the patient motion during treatment. Furthermore, the registration accuracy of

the CBCT-CBCT registration was thoroughly verified by visual inspection.

The proposed spine tracking method was tested retrospectively and online for 12 consecutive patients. However, the same exact tracking algorithm was used for both cases. For the first 4 patients, minor implementation issues were found during the online test. Therefore, a retrospective analysis was performed only for these patients. Also, the current version of the KiPSTA spine tracking application requires that the 6 DOF couch corrections are manually entered into the software; thus, requiring cooperation with therapists. For patients 5 through 8 as well as patients 10 and 11, a retrospective analysis was performed for the sessions in which online spine tracking could not be performed due to the cooperation issue.

Spinal implants were observed in 9 of 12 spine patients in this study. Interestingly, the precision of the spine tracking was better for patients with spinal implants than for those without (Fig 4C). This may be due to the implant because a good surrogate of target volume provides high image contrast that aids the registration process for spine tracking. In addition, the performance of KiPSTA was the worst for thoracic patients among the 3 patient groups. Further improvement of KiPSTA may be required for thoracic patients without spinal implant. To enhance the contrast in the region of the target vertebrae, bone DRR can be tested by thresholding intensity values in the reconstructed CBCT images. Moreover, using different image acquisition parameters may improve the image quality of kV projections.

Some angular dependency of the tracking accuracy and precision was observed for thoracic and lumbar spine patients (Fig 5). The higher accuracy and precision with anteroposterior beam angles may be explained by the relatively low attenuation compared with that with lateral beams. However, the difference in mean and SD was negligible (<0.1 mm), which demonstrates that KiPSTA performs with angular consistency. There may exist some angles at which the spine tracking method results in a relative large error, which can be improved by enhancing the quality of DRR images.

For the evaluation of spine tracking accuracy, a CBCT-CBCT registration was performed. The transformation that was obtained using Elekta XVI may also be used to calculate the ground truth translation. However, the pCT was always the reference to which CBCT images were aligned (CBCT$_{n+1}$-pCT registration) while KiPSTA is designed to capture the motion between CBCT images (CBCT$_n$-CBCT$_{n+1}$). To use the XVI couch correction for accuracy evaluation, CBCT$_n$ should be assumed to be similar to pCT. This assumption may not be satisfied when the patient offset after initial positioning is too large to be adjusted automatically due to the limited range of motion of the robotic couch. By performing a CBCT-CBCT registration, this source of uncertainty was removed. However, the existence of an uncertainty in the ground truth translation

due to the error in the CBCT-CBCT registration was still noted but expected to be negligible.

Another source of uncertainty in the accuracy evaluation of the DRR-kV projection registration may exist because the CBCT-CBCT registration only provides average patient motion between CBCT scans so any abrupt patient movement during CBCT scanning cannot be captured in the ground truth translation. This can result in an overestimation of the spine tracking error. In other words, if a patient moves during a CBCT simulation, this would result in an increase in the tracking error estimated using a single transformation matrix. Therefore, the sub-millimeter accuracy of the spine tracking algorithm can be still valid despite the existence of this uncertainty in the ground truth translation.

The estimated latency time was approximately 700 ms, which is mainly attributed to the processing time for image registration (approximately 500 ms) and largely compares with the latency time that is recommended in the study by Sharp et al.[29] However, there is a potential that this latency time can be reduced, for instance, by using graphics processing unit programming for image registration.

Conclusions

A kV projection streaming-based spine tracking method was clinically implemented and tested online during spine SRS. The sub-millimeter accuracy and precision of the proposed spine tracking method have been demonstrated. With its sub-second latency time, the proposed tracking method can be immediately used to detect patient motion between CBCT scans.

References

1. Ryu SI, Chang SD, Kim DH, et al. Image-guided hypo-fractionated stereotactic radiosurgery to spinal lesions. *Neurosurgery*. 2001;49:838-846.
2. Guckenberger M, Mantel F, Gerszten PC, et al. Safety and efficacy of stereotactic body radiotherapy as primary treatment for vertebral metastases: A multi-institutional analysis. *Radiat Oncol*. 2014;9:226.
3. Hashmi A, Guckenberger M, Kersh R, et al. Re-irradiation stereotactic body radiotherapy for spinal metastases: A multi-institutional outcome analysis. *J Neurosurg Spine*. 2016;25:646-653.
4. Foerster R, Cho BCJ, Fahim DK, et al. Histopathological findings after reirradiation compared to first irradiation of spinal bone metastases with stereotactic body radiotherapy: A cohort study [e-pub ahead of print]. *Neurosurgery*. doi:10.1093/neuros/nyy059, Accessed May 1, 2018.
5. Chang EL, Shiu AS, Lii MF, et al. Phase I clinical evaluation of near-simultaneous computed tomographic image-guided stereotactic body radiotherapy for spinal metastases. *Int J Radiat Oncol Biol Phys*. 2004;59:1288-1294.
6. Yamada Y, Bilsky MH, Lovelock DM, et al. High-dose, single-fraction image-guided intensity-modulated radiotherapy for metastatic spinal lesions. *Int J Radiat Oncol Biol Phys*. 2008;71:484-490.

7. Gibbs IC, Kamnerdsupaphon P, Ryu MR, et al. Image-guided robotic radiosurgery for spinal metastases. *Radiother Oncol*. 2007;82:185-190.

8. Gagnon GJ, Nasr NM, Liao JJ, et al. Treatment of spinal tumors using CyberKnife fractionated stereotactic radiosurgery: Pain and quality-of-life assessment after treatment in 200 patients. *Neurosurgery*. 2009;64:297-307.

9. Wu QJ, Yoo S, Kirkpatrick JP, Thongphiew D, Yin FF. Volumetric arc intensity-modulated therapy for spine body radiotherapy: Comparison with static intensity-modulated treatment. *Int J Radiat Oncol Biol Phys*. 2009;75:1596-1604.

10. Kuijper IT, Dahele M, Senan S, Verbakel WFAR. Volumetric modulated arc therapy versus conventional intensity modulated radiation therapy for stereotactic spine radiotherapy: A planning study and early clinical data. *Radiother Oncol*. 2010;94:224-228.

11. MacDougall ND, Dean C, Muirhead R. Stereotactic body radiotherapy in prostate cancer: Is rapidarc a better solution than Cyberknife? *Clin Oncol*. 2014;26:4-9.

12. Paik EK, Kim MS, Choi CW, et al. Dosimetric comparison of volumetric modulated arc therapy with robotic stereotactic radiation therapy in hepatocellular carcinoma. *Radiat Oncol J Radiat Oncol*. 2015;33:233-241.

13. Yoon K, Kwak J, Cho B, et al. Gated volumetric-modulated arc therapy vs. tumor-tracking CyberKnife radiotherapy as stereotactic body radiotherapy for hepatocellular carcinoma: A dosimetric comparison study focused on the impact of respiratory motion managements. *PLoS ONE*. 2016;11:e0166927.

14. Chuang C, Sahgal A, Lee L, et al. Effects of residual target motion for image-tracked spine radiosurgery. *Med Phys*. 2007;34:4484-4490.

15. Wang H, Shiu A, Wang C, et al. Dosimetric effect of translational and rotational errors for patients undergoing image-guided stereotactic body radiotherapy for spinal metastases. *Int J Radiat Oncol Biol Phys*. 2008;71:1261-1271.

16. Guckenberger M, Meyer J, Wilbert J, et al. Precision required for dose-escalated treatment of spinal metastases and implications for image-guided radiation therapy (IGRT). *Radiother Oncol*. 2007;84:56-63.

17. McCunniff AJ, Liang MKJ. Radiation tolerance of the cervical spinal cord. *Int J Radiat Oncol Biol Phys*. 1989;16:675-678.

18. Kirkpatrick JP, van der Kogel AJ, Schultheiss TE. Radiation dose-volume effects in the spinal cord. *Int J Radiat Oncol Biol Phys*. 2010;76:S42-S49.

19. Sahgal A, Weinberg V, Ma L, et al. Probabilities of radiation myelopathy specific to stereotactic body radiation therapy to guide safe practice. *Int J Radiat Oncol Biol Phys*. 2013;85:341-347.

20. Adler JRJ, Murphy MJ, Chang SD, Hancock SL. Image-guided robotic radiosurgery. *Neurosurgery*. 1999;44:1299-1306.

21. Hyde D, Lochray F, Korol R, et al. Spine stereotactic body radiotherapy utilizing cone-beam CT image-guidance with a robotic couch: Intrafraction motion analysis accounting for all six degrees of freedom. *Int J Radiat Oncol Biol Phys*. 2012;82:e555-e562.

22. Verbakel WFAR, Gurney-Champion OJ, Slotman BJ, Dahele M. Submillimeter spine position monitoring for stereotactic body radiotherapy using offline digital tomosynthesis. *Radiother Oncol*. 2015;115:223-228.

23. Hazelaar C, Dahele M, Mostafavi H, van der Weide L, Slotman BJ, Verbakel WFAR. Subsecond and submillimeter resolution positional verification for stereotactic irradiation of spinal lesions. *Int J Radiat Oncol Biol Phys*. 2016;94:1154-1162.

24. Rit S, Oliva MV, Brousmiche S, Labarbe R, Sarrut D, Sharp GC. The Reconstruction Toolkit (RTK), an open-source cone-beam CT reconstruction toolkit based on the Insight Toolkit (ITK). *J Phys Conf Ser*. 2014;489:012079.

25. Yoo TS, Ackerman MJ, Lorensen WE, et al. Engineering and algorithm design for an image processing Api: A technical report on ITK–the Insight Toolkit. *Stud Health Technol Inform*. 2002;85:586-592.

26. Hipwell JH, Penney GP, McLaughlin RA, et al. Intensity-based 2-D–3-D registration of cerebral angiograms. *IEEE Trans Med Imaging*. 2003;22:1417-1426.

27. Shackleford JA, Kandasamy N, Sharp GC. On developing B-spline registration algorithms for multi-core processors. *Phys Med Biol*. 2010;55:6329-6351.

28. Yoganathan SA, Maria Das KJ, Maria Midunvaleja K, et al. Evaluating the image quality of cone beam CT acquired during rotational delivery. *Br J Radiol*. 2015;88:20150425.

29. Sharp GC, Jiang SB, Shimizu S, Shirato H. Prediction of respiratory tumour motion for real-time image-guided radiotherapy. *Phys Med Biol*. 2004;49:425.